RESEARCH ARTICLE

ATMOSPHERIC SCIENCE

Global atmospheric particle formation from CERN CLOUD measurements

Eimear M. Dunne,[1]*† Hamish Gordon,[2]*‡ Andreas Kürten,[3] João Almeida,[2,3] Jonathan Duplissy,[4] Christina Williamson,[3]§ Ismael K. Ortega,[5]|| Kirsty J. Pringle,[1] Alexey Adamov,[6] Urs Baltensperger,[7] Peter Barmet,[7] Francois Benduhn,[8] Federico Bianchi,[6,7] Martin Breitenlechner,[9]¶ Antony Clarke,[10] Joachim Curtius,[3] Josef Dommen,[7] Neil M. Donahue,[11,6] Sebastian Ehrhart,[2,3] Richard C. Flagan,[12] Alessandro Franchin,[6] Roberto Guida,[2] Jani Hakala,[6] Armin Hansel,[9,13] Martin Heinritzi,[3] Tuija Jokinen,[6]# Juha Kangasluoma,[6] Jasper Kirkby,[2,3] Markku Kulmala,[6] Agnieszka Kupc,[14]§ Michael J. Lawler,[15]# Katrianne Lehtipalo,[6,7] Vladimir Makhmutov,[16] Graham Mann,[1] Serge Mathot,[2] Joonas Merikanto,[6] Pasi Miettinen,[15] Athanasios Nenes,[17,18,19] Antti Onnela,[2] Alexandru Rap,[1] Carly L. S. Reddington,[1] Francesco Riccobono,[7] Nigel A. D. Richards,[1] Matti P. Rissanen,[6] Linda Rondo,[3] Nina Sarnela,[6] Siegfried Schobesberger,[6]** Kamalika Sengupta,[1] Mario Simon,[3] Mikko Sipilä,[6] James N. Smith,[15]# Yuri Stozkhov,[16] Antonio Tomé,[20] Jasmin Tröstl,[7] Paul E. Wagner,[14] Daniela Wimmer,[3,6] Paul M. Winkler,[14] Douglas R. Worsnop,[6,21] Kenneth S. Carslaw[1]‡

Fundamental questions remain about the origin of newly formed atmospheric aerosol particles because data from laboratory measurements have been insufficient to build global models. In contrast, gas-phase chemistry models have been based on laboratory kinetics measurements for decades. We built a global model of aerosol formation by using extensive laboratory measurements of rates of nucleation involving sulfuric acid, ammonia, ions, and organic compounds conducted in the CERN CLOUD (Cosmics Leaving Outdoor Droplets) chamber. The simulations and a comparison with atmospheric observations show that nearly all nucleation throughout the present-day atmosphere involves ammonia or biogenic organic compounds, in addition to sulfuric acid. A considerable fraction of nucleation involves ions, but the relatively weak dependence on ion concentrations indicates that for the processes studied, variations in cosmic ray intensity do not appreciably affect climate through nucleation in the present-day atmosphere.

Nucleation of particles occurs throughout Earth's atmosphere by condensation of trace vapors (*1*–*3*). Around 40 to 70% of global cloud condensation nuclei (CCN) (*4*–*6*) are thought to originate as nucleated particles, so the process has a major influence on the microphysical properties of clouds and the radiative balance of the global climate system. However, laboratory measurements are needed to disentangle and quantify the processes that contribute to particle formation, and very few laboratory measurements exist under atmospheric conditions (*7*–*10*). This leaves open fundamental questions concerning the origin of particles on a global scale. First, it is not known whether nucleation is predominantly a neutral process, as assumed in most models (*11*–*13*), or whether atmospheric ions are important (*6*, *14*–*16*). This relates to the question of whether solar-modulated galactic cosmic rays (GCRs) affect aerosols, clouds, and climate (*17*–*21*). Second, the lack of measurements of nucleation rates at low temperatures means that the origin of new particles in the vast regions of the cold free troposphere has not yet been experimentally established. Third, whereas it has been shown that nucleation of sulfuric acid (H_2SO_4)–water particles in the boundary layer requires stabilizing molecules such as ammonia (NH_3), amines, or oxidized organic compounds (*7*, *8*, *22*–*24*), it is not yet known from existing experimental data over how much of the troposphere these molecules are important for nucleation. Robust atmospheric models to answer these questions need to be founded on direct measurements of nucleation rates. At present, to simulate nucleation over a very wide range of atmospheric conditions, global models must use theoretical nucleation models (*25*, *26*), which can require adjustments to the nucleation rates of several orders of magnitude to obtain reasonable agreement with ambient observations (*27*, *28*).

The lack of an experimentally based model of global particle nucleation is in stark contrast to global models of atmospheric gas-phase chemistry, which have been based on laboratory kinetics measurements since the 1970s (*29*, *30*). We built a model of the global aerosol system based on laboratory nucleation-rate measurements that is able to explain global particle concentrations without any adjustment to the rates. We derive some selected implications for CCN, cloud albedo, and hence Earth's radiative forcing.

Chamber measurements of inorganic nucleation

In Fig. 1, we present ~350 measurements of ion-induced and neutral particle formation from H_2SO_4 and NH_3 vapors, conducted in the CLOUD (Cosmics Leaving Outdoor Droplets) chamber at the CERN Proton Synchrotron. To enable globally applicable nucleation rate expressions to be developed, we combined ~250 earlier measurements (*7*, *23*, *31*) with ~100 new measurements covering a much wider range of vapor concentrations than was achieved in the previous

[1]School of Earth and Environment, University of Leeds, Leeds LS2 9JT, UK. [2]European Organization for Nuclear Research (CERN), 1211 Geneva, Switzerland. [3]Goethe-University Frankfurt am Main, Institute for Atmospheric and Environmental Sciences, Altenhöferallee 1, 60438 Frankfurt am Main, Germany. [4]Helsinki Institute of Physics, FI-00014 Helsinki, Finland. [5]Laboratoire de Physique des Lasers, Atomes et Molécules (PhLAM), Université Lille 1, UMR 8523 CNRS, 59655 Villeneuve d'Ascq, France. [6]Department of Physics, University of Helsinki, Post Office Box 64, FI-00014 Helsinki, Finland. [7]Laboratory of Atmospheric Chemistry, Paul Scherrer Institute, 5232 Villigen, Switzerland. [8]Institute for Advanced Sustainability Studies, Berliner Straße 130, D-14467 Potsdam, Germany. [9]Institute of Ion Physics and Applied Physics, Leopold-Franzens University, Technikerstraße 25, 6020 Innsbruck, Austria. [10]Department of Oceanography, University of Hawaii, 1000 Pope Road, Honolulu, HI 96822, USA. [11]Center for Atmospheric Particle Studies, Carnegie Mellon University, 5000 Forbes Avenue, Pittsburgh, PA 15213, USA. [12]Division of Chemistry and Chemical Engineering, California Institute of Technology, Pasadena, CA 91125, USA. [13]Ionicon, 6020 Innsbruck, Austria. [14]Faculty of Physics, University of Vienna, Boltzmanngaße 5, 1090 Vienna, Austria. [15]University of Eastern Finland, Post Office Box 1627, 70211 Kuopio, Finland. [16]Lebedev Physical Institute, Solar and Cosmic Ray Research Laboratory, 119991 Moscow, Russia. [17]School of Earth and Atmospheric Sciences, Georgia Institute of Technology, Atlanta, GA 30332, USA. [18]Institute of Chemical Engineering Sciences (ICE-HT), Foundation for Research and Technology, Hellas, 26504 Patras, Greece. [19]Institute for Environmental Research and Sustainable Development, National Observatory of Athens, I. Metaxa & Vas. Pavlou, 15236 Palea Penteli, Greece. [20]CENTRA-SIM, University of Lisbon and University of Beira Interior, 1749-016 Lisbon, Portugal. [21]Aerodyne Research, Billerica, MA 01821, USA.

*These authors contributed equally to this work. †Present address: Finnish Meteorological Institute, Atmospheric Research Centre of Eastern Finland, PL 1627, 70211 Kuopio, Finland. **‡Corresponding author. Email: hamish.gordon@cern.ch (H.G.); leckscc@ds.leeds.ac.uk (K.S.C.)** §Present address: Chemical Sciences Division, Earth Systems Research Laboratory, 325 Broadway, National Oceanic and Atmospheric Administration, Boulder, CO 80305, USA, and Cooperative Institute for Research in Environmental Sciences, University of Colorado, Boulder, CO 80309, USA. ||Present address: ONERA–The French Aerospace Lab, F-91123 Palaiseau, France. ¶Present address: School of Engineering and Applied Sciences, Department of Chemistry and Chemical Biology, Harvard University, Cambridge, MA 02138, USA. #Present address: Department of Chemistry, University of California, 1102 Natural Science II, Irvine, CA 92697, USA. **Present address: Department of Atmospheric Sciences, University of Washington, Seattle, WA 98195, USA.

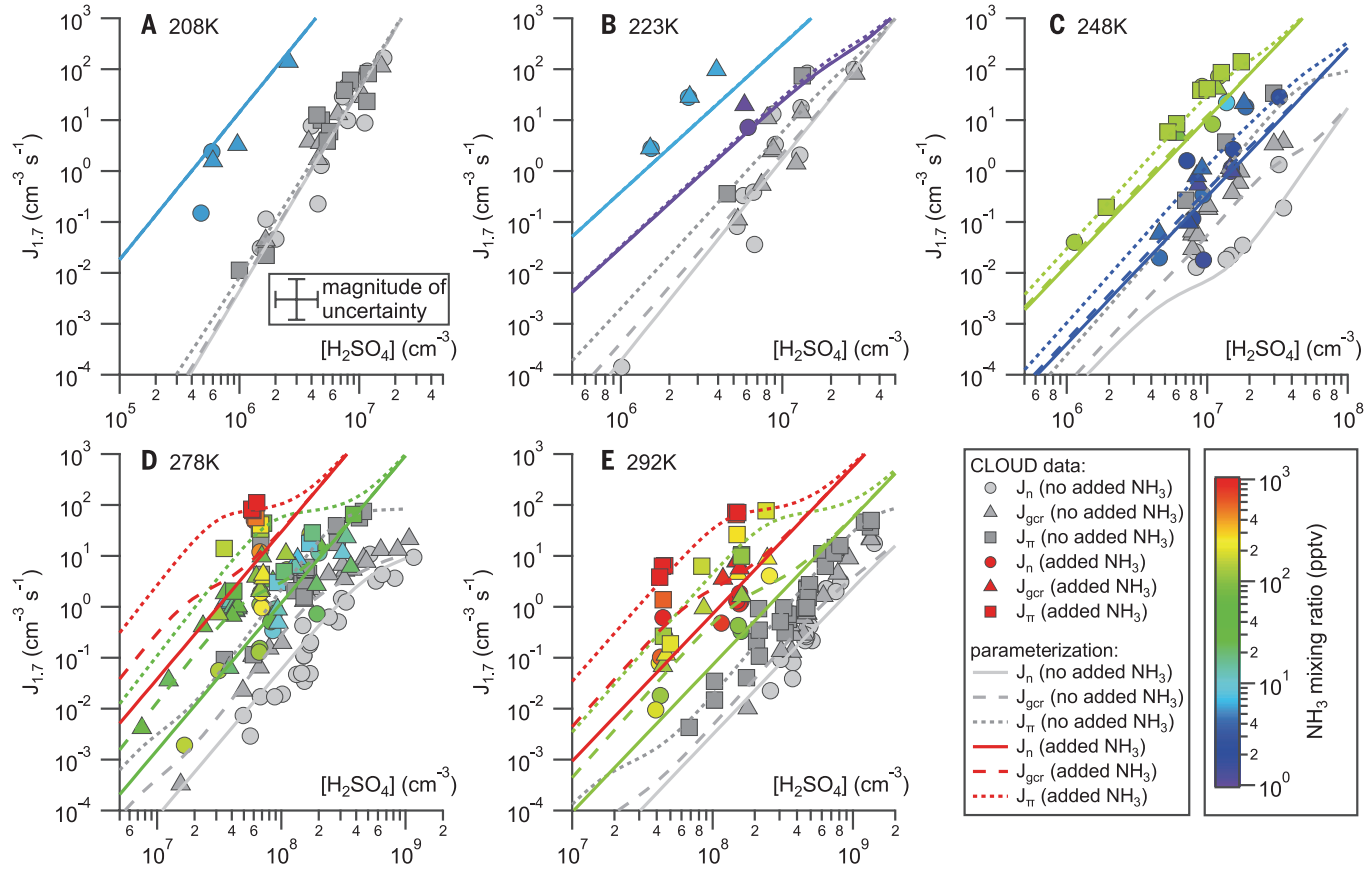

Fig. 1. Measured and parameterized nucleation rates. Neutral, GCR, and pion-beam nucleation rates (J) are shown at 1.7 nm mobility diameter as a function of sulfuric acid concentration. Rates are shown at (**A**) 208, (**B**) 223, (**C**) 248, (**D**) 278, and (**E**) 292 K. The symbols show measured values of nucleation rates: circles for neutral (n) rates (ion-pair production rate q = 0 cm^{-3} s^{-1}), triangles for GCR rates (q = 2 cm^{-3} s^{-1}), and squares for pion beam (π) rates (q ~ 75 cm^{-3} s^{-1}). The lines show parameterized nucleation rates (supplementary materials, section 8): solid lines for neutral rates, dashed lines for GCR rates, and dotted lines for pion beam rates. Gray symbols and lines indicate contaminant concentrations of NH_3 below the detection limit of the instruments (supplementary materials, section 6), whereas colored symbols and lines represent measurements at NH_3 concentrations indicated by the color scale. For clarity, the uncertainties on each data point are not shown, but the overall uncertainty of a factor of 2.5 on nucleation rate and a factor of 1.5 on [H_2SO_4] is shown separately from the real data in (A). The contaminant level of ammonia increases as temperature increases. This explains why the ionization effect without added ammonia at 292 K is smaller than that at 278 K and why the nucleation rates without added ammonia are similar at these temperatures.

experiments. We also studied ternary nucleation at temperatures as low as 208 K, typical of the upper troposphere. We combined these ~350 inorganic measurements with data on organic-mediated nucleation (*24*) to quantify nucleation rates throughout the troposphere. The experiments were performed under neutral, natural GCR and charged pion beam conditions (supplementary materials) (*32*). GCRs create ion pairs in the chamber at a rate of about 2 cm^{-3} s^{-1}, characteristic of the lower atmosphere, and the controllable pion beam is able to reproduce equilibrium ion-pair concentrations between ground level and the upper troposphere (*33*). Neutral conditions are achieved by removing ions from the chamber with an electric field.

Figure 1 shows how our full data set of inorganic nucleation rates depends on H_2SO_4, NH_3, temperature, and ionization rates. At 208 K, the nucleation rates are up to 10^4 times as high as at 248 K, the lowest temperature investigated in any previous study (*7*). The enhancement of the neutral nucleation rate caused by natural GCR ionization reaches about a factor of 15 at temperatures found in the lower troposphere. However, we measured no appreciable enhancement due to ions at lower temperatures representative of the upper troposphere, indicating that evaporation of the corresponding neutral clusters is strongly suppressed. Ammonia mixing ratios of a few parts per trillion by volume (pptv) greatly enhance the nucleation rate. For example, at 223 K, the neutral rate rises by more than a factor of 1000 when NH_3 is increased from an estimated 0.05 pptv contaminant level to 6 pptv (Fig. 1B). The negative ion cluster composition (fig. S1) (*34*) confirms that NH_3 molecules are participating in and enhancing ion-induced nucleation, although binary nucleation of sulfuric acid and water without ammonia cannot be neglected.

Although most of our measurements were conducted at 38% relative humidity (RH), the dependence of nucleation rates on RH was also measured (supplementary materials, section 9) and was found to be stronger than the dependence on ion concentrations but weaker than that on other factors. At 223 and 208 K, temperatures typical of the upper free troposphere, a change in RH between 20 and 100% induces at most a factor of 5, and typically a 50 to 100%, change in the nucleation rate, whereas ambient atmospheric concentrations of H_2SO_4 and NH_3 vary over many orders of magnitude. At 298 K, the nucleation rate increases by about a factor of 10 between 40 and 80% RH, but this does not strongly affect CCN concentrations (see the model results below).

The inorganic nucleation rates are parameterized in four dimensions—temperature, [H_2SO_4], [NH_3], and ion concentrations—and fitted to our full data set of ~350 inorganic measurements. The RH dependence was not included in the fit because of insufficient data, although we tested its effect in separate model sensitivity studies, described below. Because one of our objectives was to determine the relative importance of binary and ternary nucleation in the global atmosphere, we used the molecular composition of the charged nucleating clusters from APi-TOF (atmospheric pressure interface time-of-flight)

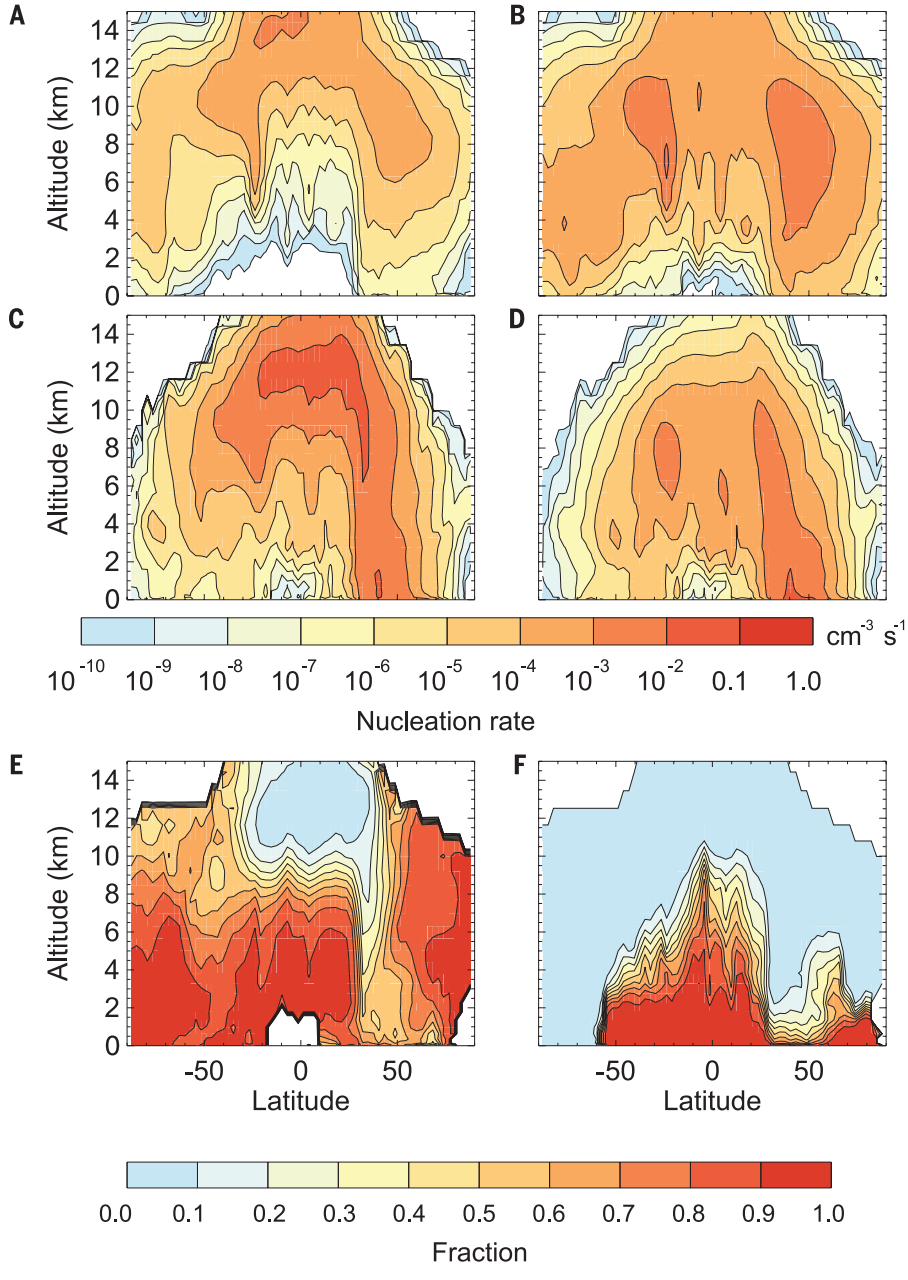

Fig. 2. Modeled zonal and annual mean particle formation rates, per cubic centimeter per second, at 3 nm diameter. (**A**) Binary (H_2SO_4-H_2O) neutral nucleation rate, (**B**) binary ion-induced nucleation rate, (**C**) ternary (H_2SO_4-NH_3-H_2O) neutral nucleation rate, (**D**) ternary ion-induced nucleation rate, (**E**) ion-induced fraction of inorganic nucleation, and (**F**) fraction of all nucleation from ternary organic nucleation (H_2SO_4-BioOxOrg-H_2O). In (E) and (F), the model data are shown only where the overall mean nucleation rate exceeds 10^{-6} cm^{-3} s^{-1}.

mass spectrometry measurements to unambiguously verify the amount of ammonia or organic species in, or their absence from, the charged nucleating clusters (*34*, *35*) (supplementary materials, section 6). Guided by these mass spectra, the four-dimensional global fit enables us to determine the dependence on trace gas concentrations and ions, even though the data are sparse in any one dimension. Over almost the full range of the measurements (supplementary materials, section 8), the nucleation rate varies approximately as $[H_2SO_4]^3$, linearly with $[NH_3]$, and linearly with ion concentration.

Global particle formation pathways

The CLOUD nucleation-rate measurements allow us, for the first time, to evaluate the global importance of competing particle sources on the basis of experimental data. The model is described in the supplementary materials, sections 11 to 16. The total nucleation rate is determined by adding the inorganic rates (previous section) to the neutral and ion-induced ternary organic H_2SO_4-BioOxOrg-H_2O nucleation rates from our earlier CLOUD chamber measurements reported in (*24*). Here BioOxOrg is a proxy for α-pinene oxidation products, and we can use the term "ternary" by treating them as a single class of vapors.

Figure 2 shows that the binary nucleation rates peak in the upper troposphere, consistent with earlier models that considered only binary neutral or ion-induced H_2SO_4-H_2O nucleation above the boundary layer (*6*, *11*–*13*). However, we find that the fractional contributions to the production rate of 3-nm-diameter particles below 15 km altitude are 15% binary (2.6% neutral and 12% ion-induced), 65% ternary inorganic with ammonia (54% neutral and 11% ion-induced), and 21% ternary organic. We are unable to quantify the fraction of ternary organic nucleation that is ion-induced as accurately as for inorganic nucleation (supplementary materials, section 15), but we estimate that 28% of all new particles are formed by ion-induced nucleation. Overall, ion-induced nucleation is the dominant process over large regions of the troposphere where particle formation rates are low. Consequently, it produces more particles than neutral nucleation in 67% of the troposphere below 15 km. Thus, almost all new particle formation over the entire troposphere involves NH_3 or organic compounds, and much of this is ion-induced.

Although our model of global nucleation rates accounts for the most important tropospheric variables, there remain some missing pieces. The most important are that we are unable to fully account for the variation of nucleation rates with RH, we do not include the contribution of amines to nucleation, and we assume that the organic nucleation rate is independent of temperature. The third of these possible sources of variation is not yet constrained by CLOUD laboratory measurements. If we assume a ternary organic rate that increases with decreasing temperature according to theoretical estimates (supplementary materials, sections 10 and 20), the ternary organic fraction of nucleation increases to 69%. This temperature dependence is likely an extreme estimate, given that terpene oxidation products are less oxidized at lower temperatures because isomerization rates are lower (*36*, *37*). This offsets the increased ease with which highly oxidized organic molecules condense at lower temperatures. An estimate of a more likely temperature dependence (supplementary materials, section 20) results in a fraction of organic nucleation of 43%. Further numerical studies of the uncertainties in the fractions of nucleation from different pathways are detailed in table S7. Because the neutral and ion-induced organic nucleation pathways have different, but unknown, dependencies on temperature (supplementary materials, section 20), the overall fraction of ion-induced nucleation is affected by this shortcoming. In the sensitivity tests in table S6, the highest fraction of ion-induced nucleation is around 63%, and the lowest is 9%.

Amines can also nucleate with sulfuric acid (*23*, *38*–*40*), but they are unlikely to influence

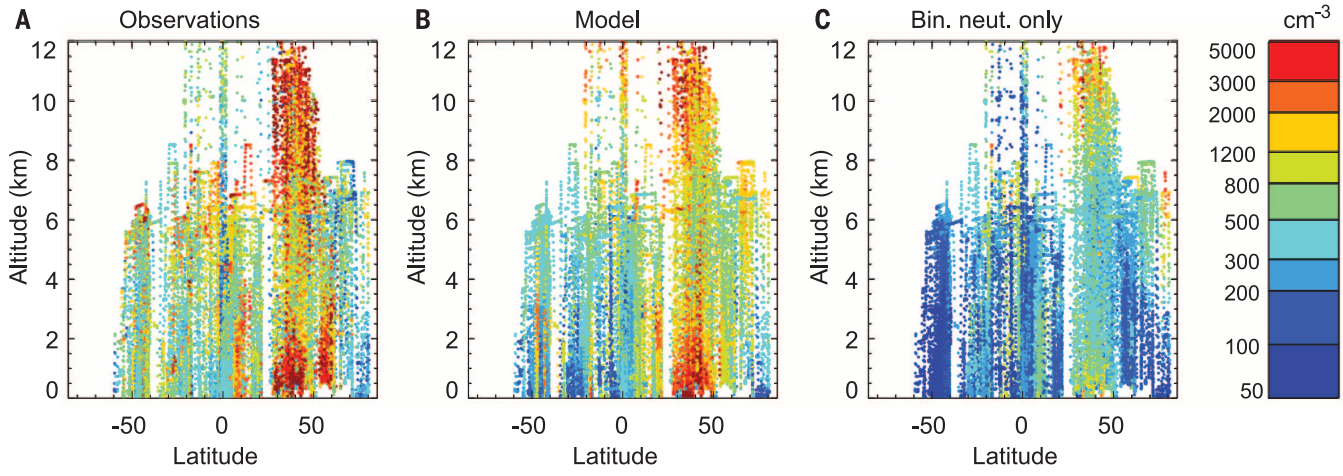

Fig. 3. Comparison of measured and modeled particle concentrations by latitude and altitude. (**A**) Measured 3-nm-diameter particle concentrations (fig. S17) (*44*). (**B**) Modeled particle concentrations (all processes). (**C**) Modeled particle concentrations including only primary particle emissions and binary neutral nucleation of sulfuric acid and water. Modeled particle concentrations in (C) are much higher than the concentrations that result from the binary-only pathway in the full model because the losses due to the condensation sink for these particles in the full model are higher than those in the binary-only model.

nucleation in the free troposphere owing to their short atmospheric lifetimes (*41*) and low fluxes. However, they are important in polluted areas of the boundary layer (*42*). A preliminary calculation (supplementary materials, section 17, and fig. S14) with a slightly different global model suggests that 6% of new particles below 500 m altitude are formed by an amine-driven mechanism, with a large uncertainty range of 3 to 27%. Amine-driven nucleation is almost certainly negligible above 500 m because of the short lifetime of amines in the atmosphere. The amine-driven nucleation has only a minimal effect on CCN concentrations (fig. S14C) because the highest amine emissions are in polluted areas with high condensation sinks, which suppress nucleation.

When we included a temperature-dependent factor to model the RH dependence of the binary nucleation rate with a polynomial function (supplementary materials, section 9), we found a 4.5% change in the concentration of 3-nm particles and a 0.3% change in the concentration of soluble 70-nm particles (approximately representative of CCN) in the troposphere up to 15 km altitude. If we assume that the ternary inorganic and organic nucleation rates depend on RH in the same way as the binary rate, we find that tropospheric 3-nm particle concentrations increase by 14%, and 70-nm particle concentrations increase by 6.5%. At cloud base level, the concentration of soluble 70-nm particles increases by 6.0%. Ternary nucleation should be less affected by RH than binary nucleation, so this change represents an upper bound. All of these numbers are comparable to typical differences between the model and observations.

Evidence from global aerosol measurements

Comparison of the global model results with atmospheric observations helps to establish how different nucleation pathways contribute to global particle concentrations. Using the simplest inorganic pathway (binary neutral nucleation) in the model systematically underestimates particle concentrations measured in the lower atmosphere and fails to explain their seasonal variation (supplementary materials, section 18). Across 35 global surface sites (*43*), including mountaintops, this binary simulation, together with primary particle emissions, can account for only 31% of the particles observed in winter in the Northern Hemisphere and 25% in summer (fig. S15). When we include ternary H_2SO_4-NH_3-H_2O nucleation, 65% of particles in winter are explained but only 36% in summer. By further including ternary H_2SO_4-BioOxOrg-H_2O nucleation, the modeled seasonal cycle of particle concentrations represents the observations well, explaining 71% of particles observed in winter and also 71% in summer. These comparisons suggest that ternary inorganic nucleation is a major source of particles in winter in the Northern Hemisphere, whereas ternary organic nucleation is a major source in summer.

We compared the predictions of the model with aircraft measurements collected at higher altitudes, a region of the atmosphere in which new particle formation is frequently modeled by binary nucleation of sulfuric acid. The aircraft campaigns (supplementary materials, section 18 and references therein) aimed to determine the most favorable chemical and meteorological conditions for nucleation in the troposphere (*44*). Relatively low model resolution prevents us from fully simulating the effects of meteorology on nucleation, especially humidity variations near clouds (*45*, *46*). Nevertheless, the full model shows good agreement with observations (Fig. 3B). In contrast, as is the case at the surface, a model with binary neutral nucleation alone can account for only 25% of the observed particle concentrations (Fig. 3C), with especially large biases of up to a factor of 5 in the lower troposphere below about 6 km altitude.

In addition to our imperfect coverage of the full parameter space of tropospheric nucleation rates, uncertainties in the model might also affect the confidence in our conclusions about the causes of global nucleation. Tables S6 and S7 summarize the principal sources of uncertainty in the CLOUD measurements and parameterization, as well as the implementation of the parameterization in the global model. The dominant sources of uncertainty, we estimate, are vapor concentrations in the model itself, rather than the parameterized nucleation rates. These and other important sources of uncertainty, such as the aerosol microphysical processes, precursor gas and primary aerosol emissions, and removal processes, have been studied comprehensively in a different configuration of this model for CCN (*47*) and 3-nm particle concentrations (*48*) by perturbing 28 model parameters in a way that allows combined uncertainties to be quantified. If we assume that the relative effect of these uncertainties on particle concentrations would be similar in the model configuration used for this study, then we can assess where we can be confident that free-tropospheric nucleation is mainly binary and where it is mainly ternary. For the southernmost remote observations in Fig. 3 [ACE-1 (Atmospheric Chemistry Experiment 1) measurements collected south of Australia; supplementary materials, section 18], the standard deviation of 3-nm particle concentrations from the 28 uncertainties is about 60% of the mean at 850 m altitude. So the binary neutral model plus one standard deviation would still lie about a factor of 5 below the observations. Although the binary model is closer to observations in some areas, such as over the Pacific Ocean, overall, its low bias relative to observations suggests that ternary nucleation (H_2SO_4 with organics or NH_3) is the primary source of

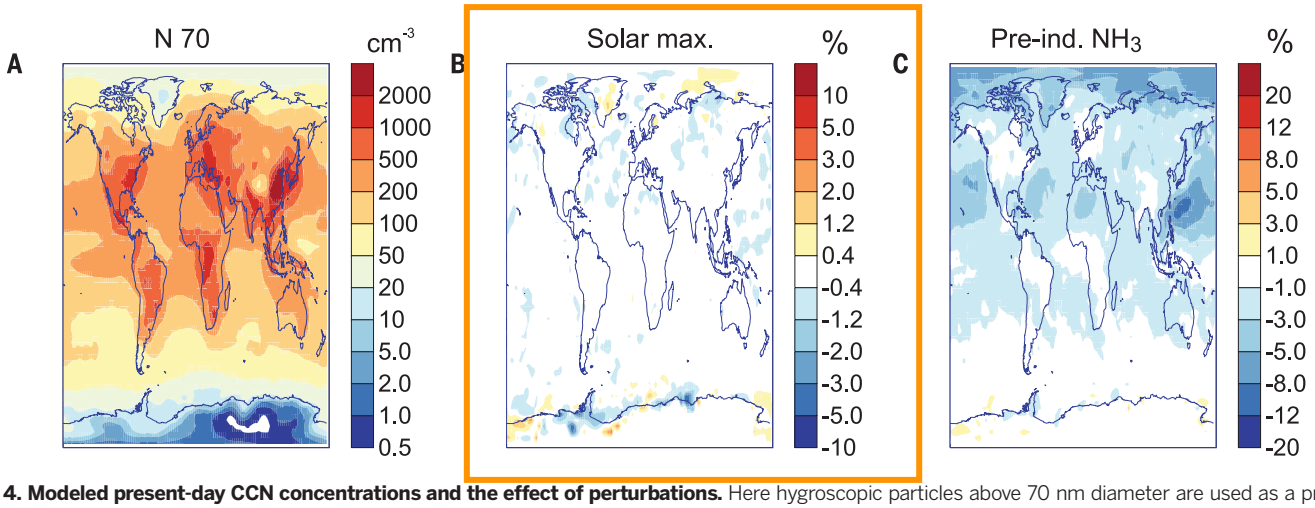

Fig. 4. Modeled present-day CCN concentrations and the effect of perturbations. Here hygroscopic particles above 70 nm diameter are used as a proxy for CCN. (**A**) Annual mean CCN concentrations at about cloud base altitude (915 hPa) (N 70, soluble particles with diameters greater than 70 nm). (**B**) Effect of changing the heliospheric modulation potential from solar minimum to maximum. (**C**) Effect of reducing ammonia concentrations to preindustrial levels. Perturbations are shown as percentage changes from the baseline shown in (A) where concentrations are higher than 5 cm^{-3}.

particles below about 6 km altitude in the environments that we have analyzed. We therefore conclude that binary nucleation becomes important only at the highest altitudes in the troposphere, and at lower altitudes, ternary nucleation dominates.

Implications for the atmosphere

The quantified effects of NH_3, oxidized organic compounds, and ions on global particle formation rates enabled us to estimate the effect on climate of changes in nucleation rates due to changing environmental conditions. We tested the effect of changes in the GCR ionization rate that occur between the solar maximum and minimum (supplementary materials, section 13) (*17*). Over the solar cycle, the global mean change in CCN at cloud base altitude (915 hPa, usually around 850 m above the surface) is only 0.1% (Fig. 4B), with local changes of no more than 1%. This is expected from the experimentally derived sublinear dependence of the inorganic nucleation rate on the ionization rate (supplementary materials, section 8) and consistent with previous assessments (*49*, *50*). The results in (*24*) suggest, with a large uncertainty, that organic nucleation is less sensitive to ionization rate than inorganic nucleation, so it would be unlikely to substantially increase the effect.

We also studied the effect of the estimated 80% increase in NH_3 emissions over the industrial period (*51*). To calculate the baseline aerosol-cloud albedo radiative forcing, we simulated preindustrial aerosols by removing anthropogenic emissions and keeping other model parameters constant, and we compared it with our present-day simulation. We then simulated present-day aerosols, keeping ammonia concentrations at preindustrial levels. In this simulation, the present-day global mean CCN concentration at cloud base level is 1.7% lower than in the usual present-day simulation (and locally up to 10 to 20% lower; Fig. 4C). Comparing the present-day simulation using preindustrial ammonia with the preindustrial simulation allows us to calculate the aerosol-cloud albedo forcing without the effect of ammonia. We can infer that ammonia has led to a strengthening of the anthropogenic aerosol-cloud radiative forcing from –0.62 to –0.66 Wm^{-2}. The 0.04 Wm^{-2} change in global mean forcing is within the uncertainty of forcing previously calculated for this model (*52*). However, the effect of ammonia on nucleation is a new process in the model, so the entire probability distribution of forcing reported in (*52*) would be shifted to lower values.

Global aerosol concentrations may be affected by future temperature changes through the temperature dependence of the formation rates. When we increase the temperatures used to calculate the inorganic nucleation rate by 2.2 K [the projected global mean change by 2100 (*53*)], mean CCN concentrations decrease by 1.0% at cloud base (locally by 10%) and cause a radiative effect of 0.02 Wm^{-2}. Therefore, a temperature-driven climate feedback related to changes in inorganic nucleation (*54*) is likely to be small compared with the large greenhouse gas forcings that are projected to occur by 2100. This result also shows that global inorganic aerosol nucleation provides a pervasive source of CCN that is relatively insensitive to environmental perturbation. The effect of rising global temperatures on organic ternary nucleation and CCN is less straightforward to calculate because there is probably compensation between decreasing nucleation rates (thus far not measured in the laboratory) and rising biogenic vapor emissions. Available observations suggest that the net effect could be to increase particle concentrations (*55*).

Conclusions

Atmospheric aerosol nucleation has been studied for over 20 years, but the difficulty of performing laboratory nucleation-rate measurements close to atmospheric conditions means that global model simulations have not been directly based on experimental data. This contrasts with the case of chemical transport modeling, which is well founded on reaction rate constants measured under controlled laboratory conditions over the past few decades (*56*). The multicomponent inorganic and organic chemical system is highly complex and is likely to be impossible to adequately represent in classical nucleation theories, just as ab initio prediction of reaction rate constants remains largely out of reach. This highlights the importance of replacing theoretical calculations with laboratory measurements, as we have done here. The CERN CLOUD measurements are the most comprehensive laboratory measurements of aerosol nucleation rates so far achieved, and the only measurements under conditions equivalent to the free and upper troposphere.

This work offers a new understanding of global particle formation as based almost entirely on ternary rather than binary nucleation, with ions playing a major but subdominant role. Our results suggest that about 43% of cloud-forming aerosol particles in the present-day atmosphere originate from nucleation, which is similar to a previous estimate of 45% obtained using the same chemical transport model and nonexperimental nucleation rates (*4*) (supplementary materials, section 16) and broadly consistent with other studies (*5*, *6*). An experimentally based model of global nucleation provides a basis for understanding how this complex system of inorganic and organic molecules responds to changes in trace gas emissions and environmental factors and, therefore, how these factors affect past and future climate.

REFERENCES AND NOTES

1. M. Kulmala *et al.*, *Atmos. Chem. Phys.* **4**, 2553–2560 (2004).
2. C. A. Brock, P. Hamill, J. C. Wilson, H. H. Jonsson, K. R. Chan, *Science* **270**, 1650–1653 (1995).
3. A. D. Clarke, *J. Atmos. Chem.* **14**, 479–488 (1992).
4. J. Merikanto, D. V. Spracklen, G. W. Mann, S. J. Pickering, K. S. Carslaw, *Atmos. Chem. Phys.* **9**, 8601–8616 (2009).
5. M. Wang, J. E. Penner, *Atmos. Chem. Phys.* **9**, 239–260 (2009).
6. F. Yu, G. Luo, *Atmos. Chem. Phys.* **9**, 7691–7710 (2009).

7. J. Kirkby *et al.*, *Nature* **476**, 429–433 (2011).
8. R. Zhang *et al.*, *Science* **304**, 1487–1490 (2004).
9. S. M. Ball, D. R. Hanson, F. L. Eisele, P. H. McMurry, *J. Geophys. Res. Atmos.* **104**, 23709–23718 (1999).
10. D. R. Benson, J. H. Yu, A. Markovich, S.-H. Lee, *Atmos. Chem. Phys.* **11**, 4755–4766 (2011).
11. R. Makkonen *et al.*, *Atmos. Chem. Phys.* **9**, 1747–1766 (2009).
12. P. J. Adams, J. H. Seinfeld, *J. Geophys. Res. Atmos.* **107**, AAC 4-1–AAC 4-23 (2002).
13. D. V. Spracklen, K. J. Pringle, K. S. Carslaw, M. P. Chipperfield, G. W. Mann, *Atmos. Chem. Phys.* **5**, 2227–2252 (2005).
14. S.-H. Lee *et al.*, *Science* **301**, 1886–1889 (2003).
15. J. Kazil *et al.*, *Atmos. Chem. Phys.* **10**, 10733–10752 (2010).
16. M. Kulmala *et al.*, *J. Aerosol Sci.* **35**, 143–176 (2004).
17. H. Svensmark, E. Friis-Christensen, *J. Atmos. Sol. Terr. Phys.* **59**, 1225–1232 (1997).
18. G. Bond *et al.*, *Science* **294**, 2130–2136 (2001).
19. U. Neff *et al.*, *Nature* **411**, 290–293 (2001).
20. K. S. Carslaw, R. G. Harrison, J. Kirkby, *Science* **298**, 1732–1737 (2002).
21. J. Kirkby, *Surv. Geophys.* **28**, 333–375 (2007).
22. M. Chen *et al.*, *Proc. Natl. Acad. Sci. U.S.A.* **109**, 18713–18718 (2012).
23. J. Almeida *et al.*, *Nature* **502**, 359–363 (2013).
24. F. Riccobono *et al.*, *Science* **344**, 717–721 (2014).
25. H. Vehkamäki *et al.*, *J. Geophys. Res. Atmos.* **107**, AAC 3-1–AAC 3-10 (2002).
26. I. Napari, M. Noppel, H. Vehkamäki, M. Kulmala, *J. Geophys. Res.* **107**, AAC 6-1–AAC 6-6 (2002).
27. S. D. D'Andrea *et al.*, *Atmos. Chem. Phys.* **13**, 11519–11534 (2013).
28. J. Jung, C. Fountoukis, P. J. Adams, S. N. Pandis, *J. Geophys. Res. Atmos.* **115**, D03203 (2010).
29. L. K. Peters, A. A. Jouvanis, *Atmos. Environ.* **13**, 1443–1462 (1979).
30. H. Rodhe, I. Isaksen, *J. Geophys. Res. Oceans* **85**, 7401–7409 (1980).
31. J. Duplissy *et al.*, *J. Geophys. Res. Atmos.* **121**, 1752–1775 (2016).
32. A. Kürten *et al.*, *J. Geophys. Res. Atmos.* 10.1002/2015JD023908 (2016).
33. A. Franchin *et al.*, *Atmos. Chem. Phys.* **15**, 7203–7216 (2015).
34. S. Schobesberger *et al.*, *Atmos. Chem. Phys.* **15**, 55–78 (2015).
35. S. Schobesberger *et al.*, *Proc. Natl. Acad. Sci. U.S.A.* **110**, 17223–17228 (2013).
36. J. D. Crounse, L. B. Nielsen, S. Jørgensen, H. G. Kjaergaard, P. O. Wennberg, *J. Phys. Chem. Lett.* **4**, 3513–3520 (2013).
37. M. Ehn *et al.*, *Nature* **506**, 476–479 (2014).
38. M. E. Erupe, A. A. Viggiano, S.-H. Lee, *Atmos. Chem. Phys.* **11**, 4767–4775 (2011).
39. C. N. Jen, P. H. McMurry, D. R. Hanson, *J. Geophys. Res. Atmos.* **119**, 7502–7514 (2014).
40. T. Bergman *et al.*, *J. Geophys. Res. Atmos.* **120**, 9606–9624 (2015).
41. X. Ge, A. S. Wexler, S. L. Clegg, *Atmos. Environ.* **45**, 561–577 (2011).
42. J. Zhao *et al.*, *Atmos. Chem. Phys.* **11**, 10823–10836 (2011).
43. D. V. Spracklen *et al.*, *Atmos. Chem. Phys.* **10**, 4775–4793 (2010).
44. A. D. Clarke, V. N. Kapustin, *J. Atmos. Sci.* **59**, 363–382 (2002).
45. A. D. Clarke *et al.*, *J. Geophys. Res. Atmos.* **103**, 16397–16409 (1998).
46. A. D. Clarke *et al.*, *J. Geophys. Res. Atmos.* **104**, 5735–5744 (1999).
47. L. A. Lee *et al.*, *Atmos. Chem. Phys.* **13**, 8879–8914 (2013).
48. K. S. Carslaw, L. A. Lee, C. L. Reddington, G. W. Mann, K. J. Pringle, *Faraday Discuss.* **165**, 495–512 (2013).
49. J. Kazil *et al.*, *Geophys. Res. Lett.* **39**, L02805 (2012).
50. J. R. Pierce, P. J. Adams, *Geophys. Res. Lett.* **36**, L09820 (2009).
51. A. F. Bouwman *et al.*, *Global Biogeochem. Cycles* **11**, 561–587 (1997).
52. K. S. Carslaw *et al.*, *Nature* **503**, 67–71 (2013).
53. U. Cubasch *et al.*, in *Climate Change 2013: The Physical Science Basis. Contribution of Working Group I to the Fifth Assessment Report of the IPCC*, T. F. Stocker *et al.*, Eds. (Cambridge Univ. Press, 2013), pp. 119–158.
54. F. Yu, G. Luo, R. P. Turco, J. A. Ogren, R. M. Yantosca, *Atmos. Chem. Phys.* **12**, 2399–2408 (2012).
55. P. Paasonen *et al.*, *Nat. Geosci.* **6**, 438–442 (2013).
56. R. Atkinson *et al.*, *Atmos. Chem. Phys.* **4**, 1461–1738 (2004).

ACKNOWLEDGMENTS

We thank CERN for supporting CLOUD with important technical and financial resources and for providing a particle beam from the CERN Proton Synchrotron. We also thank P. Carrie, L.-P. De Menezes, J. Dumollard, K. Ivanova, F. Josa, I. Krasin, R. Kristic, A. Laassiri, O. S. Maksumov, B. Marichy, H. Martinati, S. V. Mizin, R. Sitals, H. U. Walther, A. Wasem, and M. Wilhelmsson for their important contributions to the experiment. The computer modeling simulations were performed on ARC1 and ARC2, part of the high-performance computing facilities at the University of Leeds, UK. This work also made use of the POLARIS facility of the N8 High Performance Computing Centre of Excellence, provided and funded by the N8 consortium and the Engineering and Physical Sciences Research Council (grant no. EP/K000225/1). The Centre is coordinated by the Universities of Leeds and Manchester. This research has received funding from the European Commission Seventh Framework Programme [Marie Curie Initial Training Networks CLOUD- ITN (no. 215072) and CLOUD-TRAIN (no. 316662)]; European Research Council (ERC) Starting Grant no. 5736 [MOCAPAF (Role of Molecular Clusters in Atmospheric Particle Formation)] and ERC Advanced grant no. 227463 [ATMNUCLE (Atmospheric Nucleation: From Molecular to Global Scale)]; the German Federal Ministry of Education and Research (project nos. 01LK0902A and 01LK1222A); the Swiss National Science Foundation (project nos. 200020 135307 and 206620 141278); the Academy of Finland (Center of Excellence project no. 1118615 and other projects 135054, 133872, 251427, 139656, 139995, 137749, 141217, 141451, and 138951); the Finnish Funding Agency for Technology and Innovation; the V.is.l. Foundation; the Nessling Foundation; the Austrian Science Fund (FWF) (project no. J3198-N21); the Portuguese Foundation for Science and Technology (project no. CERN/FP/116387/2010); the Swedish Research Council; Vetenskapsrådet (grant 2011-5120); the Presidium of the Russian Academy of Sciences and the Russian Foundation for Basic Research (grants 08-02-91006-CERN and 12-02-91522-CERN); the U.S. National Science Foundation (grants AGS1136479, AGS1447056, AGC1439551, and CHE1012293); the U.S. Department of Energy (grant DE-SC0014469); the PEGASOS (Pan-European Gas-Aerosol-Climate Interaction Study) project funded by the European Commission under Framework Programme 7 (FP7-ENV- 2010-265148); the Davidow Foundation; and the Natural Environment Research Council project GASSP (Global Aerosol Synthesis and Science Project) under grant NE/J024252/1. We acknowledge financial support from the Royal Society Wolfson Merit Award. The nucleation rates used in our manuscript are available in the supplementary materials as a CSV file.

SUPPLEMENTARY MATERIALS

www.sciencemag.org/content/354/6316/1119/suppl/DC1
Materials and Methods
Figs. S1 to S21
Tables S1 to S7
References (*57*–*135*)
Data S1

18 January 2016; accepted 12 October 2016
Published online 27 October 2016
10.1126/science.aaf2649

REPORTS

TOPOLOGICAL MATTER

Quantized Faraday and Kerr rotation and axion electrodynamics of a 3D topological insulator

Liang Wu,[1]*† M. Salehi,[2] N. Koirala,[3] J. Moon,[3] S. Oh,[3] N. P. Armitage[1]*

Topological insulators have been proposed to be best characterized as bulk magnetoelectric materials that show response functions quantized in terms of fundamental physical constants. Here, we lower the chemical potential of three-dimensional (3D) Bi_2Se_3 films to ~30 meV above the Dirac point and probe their low-energy electrodynamic response in the presence of magnetic fields with high-precision time-domain terahertz polarimetry. For fields higher than 5 tesla, we observed quantized Faraday and Kerr rotations, whereas the dc transport is still semiclassical. A nontrivial Berry's phase offset to these values gives evidence for axion electrodynamics and the topological magnetoelectric effect. The time structure used in these measurements allows a direct measure of the fine-structure constant based on a topological invariant of a solid-state system.

Topological phenomena in condensed matter physics provide some of the most precise measurements of fundamental physical constants. The measurement of the quantum conductance $G_{xy} = e^2/h$ from the quantum Hall effect (*1*) and the flux quantum from the Josephson effect (*2*, *3*) provide the most precise value for Planck's constant h. More recently, topological insulators have been discovered (*4*–*6*), in which topological properties of the bulk wave functions give rise to a topologically protected surface metal with a massless Dirac spectrum. It has been proposed that topological insulators are best characterized not as surface conductors but as bulk magnetoelectrics (*7*, *8*) with a quantized magnetoelectric response coefficient whose size is set by the fine-structure constant $\alpha = e^2/2\varepsilon_0 hc$. Such a measurement could provide precise values for three fundamental physical constants: the electric charge e, Planck's constant h, and the vacuum impedance $Z_0 = \sqrt{\mu_0/\varepsilon_0}$ in a solid-state context.

Magnetoelectrics (ME) are materials in which a polarization can be created by an applied magnetic field or a magnetization can be created by an applied electric field (*9*); representative examples are Cr_2O_3 (*10*) with an ME coupling of the $\boldsymbol{E}\cdot\boldsymbol{B}$ form and multiferroic $BiFeO_3$ (*11*), where the ME coupling can be expressed (in part) in a $\boldsymbol{E} \times \boldsymbol{B}$

[1]Institute for Quantum Matter, Department of Physics and Astronomy, The Johns Hopkins University, Baltimore, MD 21218, USA. [2]Department of Materials Science and Engineering, Rutgers, The State University of New Jersey, Piscataway, NJ 08854, USA. [3]Department of Physics and Astronomy, Rutgers, The State University of New Jersey, Piscataway, NJ 08854, USA.
***Corresponding author. Email: liangwu@berkeley.edu (L.W.); npa@jhu.edu (N.P.A.)** †Present address: Department of Physics, University of California, Berkeley, Berkeley, CA 94720, USA.

Science

Global atmospheric particle formation from CERN CLOUD measurements

Eimear M. Dunne, Hamish Gordon, Andreas Kürten, João Almeida, Jonathan Duplissy, Christina Williamson, Ismael K. Ortega, Kirsty J. Pringle, Alexey Adamov, Urs Baltensperger, Peter Barmet, Francois Benduhn, Federico Bianchi, Martin Breitenlechner, Antony Clarke, Joachim Curtius, Josef Dommen, Neil M. Donahue, Sebastian Ehrhart, Richard C. Flagan, Alessandro Franchin, Roberto Guida, Jani Hakala, Armin Hansel, Martin Heinritzi, Tuija Jokinen, Juha Kangasluoma, Jasper Kirkby, Markku Kulmala, Agnieszka Kupc, Michael J. Lawler, Katrianne Lehtipalo, Vladimir Makhmutov, Graham Mann, Serge Mathot, Joonas Merikanto, Pasi Miettinen, Athanasios Nenes, Antti Onnela, Alexandru Rap, Carly L. S. Reddington, Francesco Riccobono, Nigel A. D. Richards, Matti P. Rissanen, Linda Rondo, Nina Sarnela, Siegfried Schobesberger, Kamalika Sengupta, Mario Simon, Mikko Sipilä, James N. Smith, Yuri Stozkhov, Antonio Tomé, Jasmin Tröstl, Paul E. Wagner, Daniela Wimmer, Paul M. Winkler, Douglas R. Worsnop and Kenneth S. Carslaw

Science **354** (6316), 1119-1124.
DOI: 10.1126/science.aaf2649originally published online October 27, 2016

How new particles form

New particle formation in the atmosphere produces around half of the cloud condensation nuclei that seed cloud droplets. Such particles have a pivotal role in determining the properties of clouds and the global radiation balance. Dunne *et al.* used the CLOUD (Cosmics Leaving Outdoor Droplets) chamber at CERN to construct a model of aerosol formation based on laboratory-measured nucleation rates. They found that nearly all nucleation involves either ammonia or biogenic organic compounds. Furthermore, in the present-day atmosphere, cosmic ray intensity cannot meaningfully affect climate via nucleation.

Science, this issue p. 1119